Ultralow Absorption Coefficient and Temperature Dependence of Radiative Recombination of CH3NH3PbI3 Perovskite from Photoluminescence

ARTICLE *in* JOURNAL OF PHYSICAL CHEMISTRY LETTERS · FEBRUARY 2015

Impact Factor: 7.46 · DOI: 10.1021/acs.jpclett.5b00044

THE JOURNAL OF PHYSICAL CHEMISTRY Letters

Letter

pubs.acs.org/JPCL

Ultralow Absorption Coefficient and Temperature Dependence of Radiative Recombination of $CH_3NH_3PbI_3$ Perovskite from Photoluminescence

Chog Barugkin, Jinjin Cong, The Duong, Shakir Rahman, Hieu T. Nguyen, Daniel Macdonald, Thomas P. White, and Kylie R. Catchpole*

Research School of Engineering, The Australian National University, Canberra, Australia 2601

Supporting Information

ABSTRACT: Spectrally resolved photoluminescence is used to measure the band-to-band absorption coefficient $\alpha_{BB}(\hbar\omega)$ of organic−inorganic hybrid perovskite methylammonium lead iodide ($CH_3NH_3PbI_3$) films from 675 to 1400 nm. Unlike other methods used to extract the absorption coefficient, photoluminescence is only affected by band-to-band absorption and is capable of detecting absorption events at very low energy levels. Absorption coefficients as low as 10^{-14} cm^{-1} are detected at room temperature for long wavelengths, which is 14 orders of magnitude lower than reported values at shorter wavelengths. The temperature dependence of $\alpha_{BB}(\hbar\omega)$ is calculated from the photoluminescence spectra of $CH_3NH_3PbI_3$ in the temperature range 80−360 K. Based on the temperature-dependent $\alpha_{BB}(\hbar\omega)$, the product of the radiative recombination coefficient and square of the intrinsic carrier density, $B(T) \times n_i^2$, is also obtained.

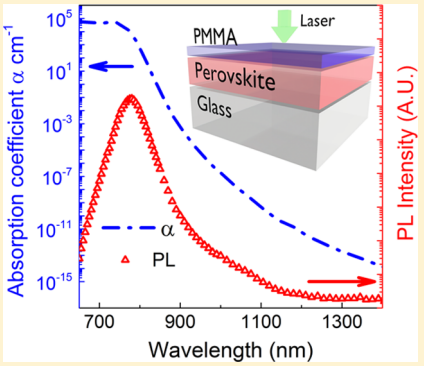

As an emerging technology in photovoltaics (PV), the rapid development of organic−inorganic halide perovskite-based solar cells has attracted enormous interest from the entire PV community. Kojima et al. reported the first photovoltaic function of the organic−inorganic halide perovskite compounds $CH_3NH_3PbBr_3$ and $CH_3NH_3PbI_3$.[1] Since then, tremendous progress has been made to improve the power conversion efficiency of perovskite solar cells from 3.8% in 2009[1] to 19.3% in 2014.[2] Very recently, researchers from KRICT have achieved a new record with the certification of a nonstabilized efficiency of 20.1%.[3]

Perovskite solar cells are promising for mass production because they have important properties such as low-cost materials, simple fabrication process, and high efficiency. Compared to existing solar cells technologies, perovskites have advantages over conventional materials such as stronger absorption, which allows the fabrication of thinner cell structures.[4] Very low fundamental energy loss allows the potential for achieving high open circuit voltage, as perovskites have very low nonradiative recombination rates. Another remarkable property of perovskite is the combination of high band gap and sharp absorption edge.[4,5] The absorption coefficient of $CH_3NH_3PbI_3$ has a clear exponential reduction below the band edge without any obvious deep states.[5,6] These features together with the optical band gap (1.55 eV) and high power conversion efficiency make perovskite a promising material candidate for the top solar cell of a crystalline silicon based tandem structure.[7−9]

As one of the most important fundamental properties of any type of semiconductor, the absorption coefficient of $CH_3NH_3PbI_3$ is reported in several publications.[5,6] For any solar cell, knowledge of the absorption coefficient in the spectral region where the absorber is deemed to be active is of extreme importance. Xing et al. calculated the absorption coefficient based on the optical transmittance and reflectance of a $CH_3NH_3PbI_3$ film on a quartz substrate.[6] Such measurements provide useful information but do not allow band-to-band absorption to be separated from parasitic absorption. De Wolf et al. extended the coefficient data to the sub-band gap region with Fourier-transform photocurrent spectroscopy (FTPS), a technique that can obtain the absorptance of the active layer without any substrate contribution.[5] However, these techniques do not have sufficient sensitivity to measure the absorption coefficient of $CH_3NH_3PbI_3$ in the very long wavelength region, where the absorption properties are important to potential applications in tandem cell structures.[8] This has motivated recent efforts to accurately determine the optical constants for perovskites, as these values are essential for correct optical design of devices.[10,11] Supported by the published absorption coefficient data, the first perovskite and silicon tandem structures were simulated.[9,12] However, these works do not consider long wavelength parasitic absorption, as such data was not yet available. This leads us to the application of photoluminescence (PL) spectroscopy to determine the absorption coefficient of $CH_3NH_3PbI_3$ perovskite film.

Received: January 9, 2015
Accepted: February 10, 2015

DOI: 10.1021/acs.jpclett.5b00044
J. Phys. Chem. Lett. 2015, 6, 767−772

PL is a widely used characterization tool for silicon-based photovoltaic applications such as determining minority carrier lifetime,[13] studying silicon defects,[14] and extracting band-to-band absorptance.[15−17] From the band-to-band absorptance extracted from photoluminescence spectra (PLS) of silicon materials, the absorption coefficient of silicon can also be accurately determined to very low values (as low as 10^{-16} cm^{-1}), which other techniques cannot achieve.[15,18] The photon-excited spontaneous emission from a semiconductor material is defined by Würfel via the generalized Planck radiation law,[19] and has been validated for both direct[20] and indirect[21] transitions. As PL in a certain energy interval is the reverse process of interband absorption of a photon, it is only sensitive to band-to-band absorption, without any disturbance from free carriers and parasitic absorption.[15,19] The relationship between the band-to-band absorption coefficient $\alpha_{BB}(\hbar\omega)$ and the spontaneous emission rate $dr_{em}(\hbar\omega)$ from a volume element into a solid angle Ω per energy interval $d\hbar\omega$ is described by[15]

$$dr_{em}(\hbar\omega) = \alpha_{BB}(\hbar\omega)\frac{c_\gamma D_\gamma \Omega}{\exp\left(\frac{\hbar\omega - \mu_\gamma}{kT}\right) - 1} d\hbar\omega \quad (1)$$

c_γ is the velocity of light in the emitting medium with refractive index n, $D_\gamma = n^3(\hbar\omega)^2/(4\pi^3\hbar^3c_o^3)$ is the density of states per solid angle for photons in the medium, and $\hbar$ is the reduced Planck constant. μ_γ refers to the chemical potential of the emitted photons (equal to the difference of the quasi-Fermi energies, $\varepsilon_{F,C}-\varepsilon_{F,V}$), k is Boltzmann's constant, and T is the absolute temperature of the sample. To obtain a measurable quantity, the emission rate has to be converted into emitted photon current. By integrating the emission rate over the sample thickness and taking reabsorption and reflections at both surfaces into account, we can determine the emitted photon flux outside a planar sample. If the electrons and holes are distributed homogeneously through the sample (i.e., for long diffusion lengths and low surface recombination), the photon current density $dj_e(\hbar\omega)$ emitted in the interval $d\hbar\omega$ of hemispherical space outside of the sample is found to be[15,16,22,23]

$$dj_e(\hbar\omega) \propto A_{BB}(\hbar\omega)\cdot(\hbar\omega)^2\cdot\exp\left(-\frac{\hbar\omega}{kT}\right) \quad (2)$$

with $A_{BB}(\hbar\omega)$ being the band-to-band absorptance in the active layer. The relationship between absorptance and the absorption coefficient $\alpha_{BB}(\hbar\omega)$ becomes[15]

$$A_{BB}(\hbar\omega) = [1 - R(\hbar\omega)]\frac{1 - \exp[-\alpha_{BB}(\hbar\omega)d]}{1 - R(\hbar\omega)\exp[-\alpha_{BB}(\hbar\omega)d]} \quad (3)$$

where d is the sample thickness, and $R(\hbar\omega)$ is the sample reflectivity. In the long wavelength region where the absorption is weak, $\alpha_{BB}(\hbar\omega)$ can be derived from $dj_e(\hbar\omega)$ via the following equation:[15]

$$dj_e(\hbar\omega) \propto \alpha_{BB}(\hbar\omega)\cdot(\hbar\omega)^2\cdot\exp\left(-\frac{\hbar\omega}{kT}\right) \quad (4)$$

i.e., for the weakly absorbed part of the spectrum, where $\alpha_{BB}(\hbar\omega)d \ll 1$, extraction of $\alpha_{BB}(\hbar\omega)$ by using eq 4 is strictly valid, regardless of the distribution of electrons and holes and the surface reflectance.[24]

In this study, the PL spectrum of a solution-processed $CH_3NH_3PbI_3$ film has been measured at room temperature from 650 to 1400 nm. Poly(methyl methacrylate) (PMMA) is used to prevent the degradation of $CH_3NH_3PbI_3$ film during the measurement. The diffusion length of $CH_3NH_3PbI_3$ is typically on the order of 100 nm,[6] which means the diffusion length of our sample is likely to be similar to the sample thickness. We therefore assume that it is reasonable to approximate the carrier density to be uniform depth-wise across the sample, and we use eqs 2 and 3 to determine the band-to-band absorption coefficient of $CH_3NH_3PbI_3$ from the PL spectra. Note that we find good agreement with previously published absorption coefficient data over the wavelength range where data is available, indicating that this assumption of approximately uniform carrier profiles is reasonable. For the long wavelength region where there is no previously published data, absorption is very weak, and eq 4 is valid. We therefore use this approach to extend our results to absorption coefficient values down to 10^{-14} cm^{-1}.

We also perform PLS measurements on a $CH_3NH_3PbI_3$ film at different temperatures ranging from 80 to 360 K to obtain temperature-dependent absorption coefficient data from 650 to 900 nm. Finally, we use the extracted $\alpha_{BB}(\hbar\omega)$ at different temperatures to determine the product of the radiative recombination coefficient and the square of the intrinsic carrier density $B(T) \times n_i^2$ in a temperature range of 80−360 K.

The solution-based fabrication process of $CH_3NH_3PbI_3$ films is carried out at room temperature with N_2 ambient. PbI_2 (99%, Sigma-Aldrich) is dissolved in dimethylformamide (DMF) at 461 mg/mL and heated to 60 °C with agitation. The PbI_2 solution is spin-coated on 25 × 25 mm glass microscope slides at 3000 rpm for 15s and dried for several minutes. Then 0.5 mL of methylammonium iodide (Dyesol) solution (10 mg/mL in isopropanol) is deposited dynamically over several seconds onto the PbI_2 substrates spinning at 3000 rpm for 30 s. The substrates are heated on a hot plate at 100 °C for 10 min to form the $CH_3NH_3PbI_3$ film. We find that this process can reliably produce $CH_3NH_3PbI_3$ films of ∼300 nm thickness. For the PLS measurements, a layer of PMMA is spin-coated at 4000 rpm for 30 s on top of the perovskite film followed by a 5 min bake at 120 °C.

To measure the PL emission spectra of the $CH_3NH_3PbI_3$ films, we illuminate the sample with a laser source powered by a 532 nm free running diode at normal incidence with 16 mW intensity on the sample, and a spot diameter of approximately 3 mm. The intensity of the laser was carefully selected to maximize the PL emission signal while preventing degradation during the measurement. Moisture-induced degradation of perovskite film with laser exposure has been observed by others.[25] With a PMMA capping layer, the perovskite films can stay up to 2 h under the illumination without obvious degradation. A 532 nm band-pass filter is used to achieve a clean excitation line. The emitted radiation is focused and transmitted into a double-grating monochromator with 600 grooves/mm and 1000 nm blaze. The emission spectrum at 650−900 nm is detected with a photomultiplier detector, and the spectrum at 900−1400 nm is captured with a liquid nitrogen-cooled InGaAs detector. A long pass filter is used to prevent any laser light reaching the detector. The reasons for using two different detectors to measure different sections of the spectrum are as follows: First, the spectral responses of both detectors have limitations in terms of their sensitivity; neither detector is capable of measuring the entire 650 nm to

DOI: 10.1021/acs.jpclett.5b00044
J. Phys. Chem. Lett. 2015, 6, 767−772

1400 nm spectrum independently. Second, the emission above 900 nm is very weak, so a mechanical chopper and lock-in amplifier is used with the InGaAs detector to improve the signal-to-noise ratio. In order to sensitively measure the emitted luminescence signal at very long wavelength range, the spectrum from 900 to 1400 nm is measured in two sections with different amplifications to make sure the weakest signal is still measurable. The first part is measured from 850 to 1050 nm, then the second section of spectrum with increased amplification is measured from 1000 to 1400 nm. The three spectra (650−900 nm, 850−1050 nm, and 1000−1400 nm) are stitched together to form a single spectrum from 650 to 1400 nm (shown in Figure 1) based on the "sum of square error"

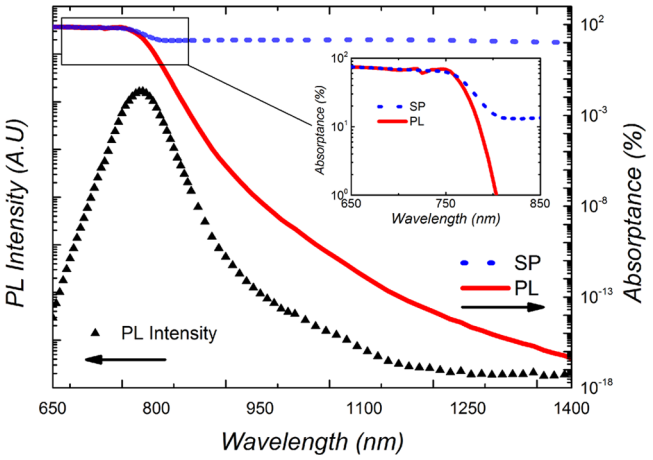

Figure 1. PL spectra of 300 nm perovskite $CH_3NH_3PbI_3$ film (left *Y*-axis). Spectrophotometer-measured absorptance (blue dash line) and PL extracted absorptance of $CH_3NH_3PbI_3$ (red solid line) as a function of wavelength (right *Y*-axis).

method applied to the overlapping regions.[18] We also used a PerkinElmer 1050 spectrophotometer with integrating sphere detector to measure the reflectance $R(\hbar\omega)$ and transmittance $T(\hbar\omega)$ of the samples in the wavelength range of 650 to 1400 nm. The overall absorptance of the sample is then calculated as $A(\hbar\omega) = 1 - R(\hbar\omega) - T(\hbar\omega)$.

To capture the PL spectra of a $CH_3NH_3PbI_3$ film at various temperatures, the sample is kept in a liquid-nitrogen-cooled cryostat with temperature variation of less than 0.1 K. The measurement is taken at 10 K intervals from 650 to 900 nm with the photomultiplier detector in a temperature range of 80−360 K, which covers the phase transition point of $CH_3NH_3PbI_3$ and the entire device operating temperature.[26,27]

We extract the relative absorptance $A_{BB}(\hbar\omega)$ from PL spectra based on eq 2.[15,19,20] The PL spectra can be divided by $\hbar\omega^2 \exp(-\hbar\omega/kT)$ to obtain the relative $A_{BB}(\hbar\omega)$ of the sample as a function of wavelength (Figure 1). The absorptance that we extract is only relative, as the PL is measured in arbitrary units. $A_{BB}(\hbar\omega)$ is then normalized to $1 - R(\hbar\omega)$ at a wavelength above the bandgap (675 nm) to convert into absolute values, where $R(\hbar\omega)$ is the front surface reflectance measured with the spectrophotometer.

As shown in Figure 1, black triangle points corresponding to the left *Y*-axis represent the PL spectra of $CH_3NH_3PbI_3$ film at room temperature. The red solid line corresponding to the secondary *Y*-axis is $A_{BB}(\hbar\omega)$ extracted from the PL spectra and normalized to the blue dash line (spectrophotometer (SP)-measured absorptance (A)) at a wavelength of 675 nm. $A_{BB}(\hbar\omega)$ decays to a very low value of 10^{-16} at 1400 nm, whereas the value measured with the spectrophotometer remains above 10^{-1} from 800 to 1400 nm. The higher value of SP-measured absorptance at long wavelength could be due to parasitic absorption or to the scattered light being trapped within the glass substrate and escaping out of the integrating sphere. In contrast with the SP measurements, the absorptance extracted from PL does not depend on parasitic or free carrier absorption in any layer of the structure. It only detects the emission associated from the band-to-band absorption in perovskite film. Therefore, any absorption that does not contribute to photocurrent generation is ignored, which allows us to sensitively measure the band-to-band absorptance in the active layer at very low energy levels.

The absorption coefficient can be derived from the absorptance using eq 3. We assume the same reflectivity $R(\hbar\omega)$ for both surfaces of the 300 nm thick sample. The extracted absorption coefficient of $CH_3NH_3PbI_3$ for the wavelength range 650−1400 nm at room temperature (295 K) is presented in Figure 2. As a comparison, we include the

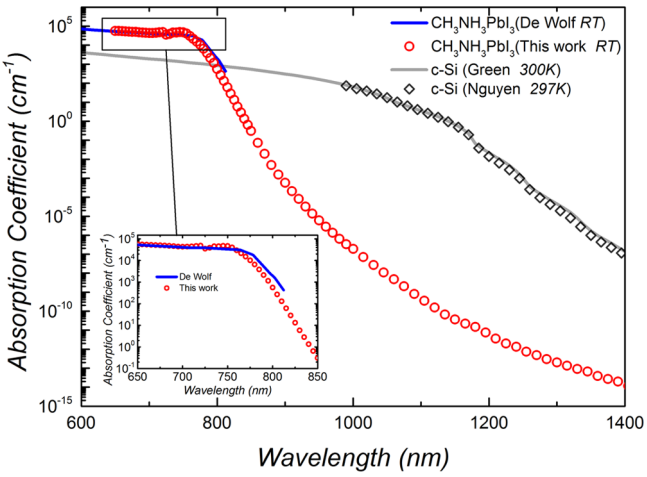

Figure 2. Absorption coefficient of $CH_3NH_3PbI_3$ obtained from a PL spectrum at room temperature (RT; red line). As a comparison, we plot $\alpha_{BB}(\hbar\omega)$ of $CH_3NH_3PbI_3$ (blue line) obtained by FTPS by De Wolf et al.[5] and $\alpha(\hbar\omega)$ of c-Si (black line) obtained by Green et al. from transmittance/reflectance measurements of intrinsic silicon and spectral-response measurements on high-efficiency solar cells,[28,29] and $\alpha_{BB}(\hbar\omega)$ of c-Si (black diamond) obtained from PL spectra by Nguyen et al.[18]

absorption coefficient of $CH_3NH_3PbI_3$ reported by De Wolf[5] (obtained by digitizing the published data), and two sets of absorption coefficient of c-Si obtained by Green[28,29] and Nguyen et al.,[18] respectively. Our absorption coefficient matches very well with De Wolf and co-workers' results in the wavelength range shorter than the band gap. In the sub band gap region, both spectra have a very sharp absorption edge, and the slopes of the two spectra are much steeper than that of c-Si. The absorption coefficient of $CH_3NH_3PbI_3$ film calculated by the PL technique can extend to a wavelength of 1400 nm with a value as small as 10^{-14} cm^{-1}. The strong exponential decay of the absorption coefficient clearly indicates high structural order and low density of optical deep states in the $CH_3NH_3PbI_3$ film.[5] As a result, solar cells made with this material should be able to achieve a high open circuit voltage, which is beneficial for a top cell in a tandem structure.

DOI: 10.1021/acs.jpclett.5b00044
J. Phys. Chem. Lett. 2015, 6, 767−772

In a recent study of the absorption coefficient of $CH_3NH_3PbI_3$, De Wolf et al.[5] reported the presence of an Urbach tail, evident as a straight line over 4 orders of magnitude when plotted on a logarithmic scale; this work shows this behavior extending over more than 8 orders of magnitude, up to a wavelength of 900 nm. The slope of the absorption coefficient deviates from the expected straight line dependence at higher wavelengths. The reason for this deviation will be the subject of further studies.

In the weak absorption region $\alpha_{BB}(\hbar\omega)d \ll 1$ ($\lambda \geq$ 800 nm), eq 4 can be used to extract the absorption coefficient accurately, as the PL spectra does not depend on the distribution of electrons and holes, or the surface reflectance because photon reabsorption can be neglected.[15] Since this equation also provides only relative values, the use of eq 4 requires a previously obtained value of α_{BB} at one wavelength for normalization. We use the value of α_{BB} at λ = 800 nm using eq 2 to provide normalization. With this normalization, eq 2 and eq 4 give the same results for the region $\alpha_{BB}(\hbar\omega)d \ll 1$ ($\lambda \geq$ 800 nm). This is because, for weak absorption, $A_{BB} \propto \alpha_{BB}$. To verify this, we extract the absorption coefficient in the wavelength range of weak absorption based on eq 4 and compare the absorption coefficient with the values calculated from eqs 2 and 3. The results agree very closely (see Supporting Information Figure S1). We conclude that the relative values of $\alpha_{BB}(\hbar\omega)$ are accurate beyond $\lambda \geq$ 800 nm because they do not require any assumptions about the diffusion length of the sample. In addition, the agreement with the data of De Wolf et al. indicates that the data for $\lambda <$ 800 nm is accurate. Nevertheless, more accurate results could be obtained by applying the same technique to samples with longer diffusion length.

The temperature dependence of the PL spectra of $CH_3NH_3PbI_xCl_{3-x}$ film has been examined and reported in the literature.[30] In the present study, with very good temperature fluctuation control (less than 0.1 K), the measurement of PL spectra of $CH_3NH_3PbI_3$ is carried out from 80 K to 360 K in 10 K increments. Five of the spectra are presented in Figure 3, normalized to unity at the peak value to allow for direct comparison. This shows the emission peaks narrowing with decreasing temperature from 350 to 240 K with a clear red-shift of the short-wavelength side of the peaks. This peak narrowing upon cooling can be explained by the fact that with lower temperature the charge carriers have less thermal energy and are therefore located closer to the band edges. With further reduction of the temperature, the peaks broaden again and start to show a contribution from a secondary peak close to 800 nm. The resolution of two excitonic peaks in the PL spectra below 160 K has been reported previously, and is explained as the transition from the orthorhombic phase to the tetragonal phase.[26,30] This secondary peak vanishes, and the widths of the PL spectra get narrower as the temperature increases.

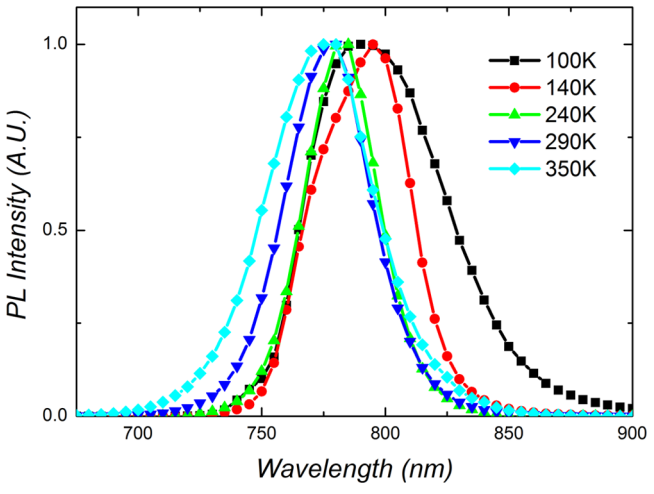

Figure 3. PL spectra of $CH_3NH_3PbI_3$ measured at different temperatures are shown as a function of wavelength (normalized to 1 at the peak of each spectra).

Using the same method as in the previous section, the relative absorptance of $CH_3NH_3PbI_3$ film is extracted from the PL spectra measured at different temperatures. As the absorptance spectra extracted from PL are relative values, normalization has to be applied to convert the absorptance into absolute values in order to calculate the absolute absorption coefficient. To convert the relative value to an absolute value, at least one absolute absorptance point at high energy range has to be known for each temperature. The room-temperature absorptance can be measured with the spectrophotometer, but the absolute absorptance at any other temperature is not known. However, as the optical band gap of $CH_3NH_3PbI_3$ is at wavelengths >700 nm for the temperature range from 80 to 360 K, the absorptance of $CH_3NH_3PbI_3$ at wavelengths <700 nm should be saturated in this temperature range and, to a good approximation, be similar in magnitude to the absorptance at room temperature. Based on this assumption, we normalize the relative absorptance of $CH_3NH_3PbI_3$ at each different temperature to the absorptance measured with the spectrophotometer at room temperature at 700 nm. Once the absolute absorptance at different temperatures is obtained, the corresponding absorption coefficient of $CH_3NH_3PbI_3$ film is extracted with eq 3 as shown in Figure 4.

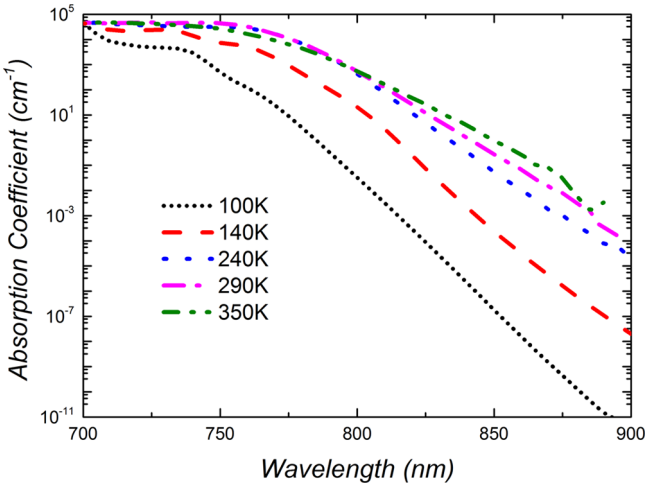

Figure 4. Temperature-dependent absorption coefficient of $CH_3NH_3PbI_3$ extracted from PL spectra.

From Figure 4, we can see that the temperature of $CH_3NH_3PbI_3$ has a strong impact on its absorption properties. The absorption coefficient measured at lower temperature has clear humps originating from the stronger exciton−phonon interaction. These features may also be associated with a phase change in the $CH_3NH_3PbI_3$ film, which occurs at approximately 160 K.[26,30] A detailed explanation of these effects requires

DOI: 10.1021/acs.jpclett.5b00044
J. Phys. Chem. Lett. 2015, 6, 767−772

further experimental investigation. With increasing temperature, the humps disappear, and the absolute value of the absorption coefficient at long wavelengths increases significantly. When the temperature reaches 350 K and above, the absorption coefficient starts to decrease at the band gap region due to the blue shift of the band gap, while in the sub band gap region the absorption coefficient continues to increase with rising temperature.

Obtaining the temperature-dependent $\alpha_{BB}(\hbar\omega)$ also allows us to calculate the radiative recombination coefficient of perovskite $CH_3NH_3PbI_3$, which is also a crucial property to understand and simulate the photovoltaic behavior of perovskite solar cells. The radiative recombination coefficient $B(T)$ of a semiconductor at a given temperature is calculated as[22,31]

$$B(T) = \frac{1}{n_i^2} \times \frac{1}{\pi^2\hbar^3 c_0^2} \int_0^\infty \left[n^2 \times (\hbar\omega)^2 \times \alpha_{BB}(\hbar\omega, T) \times \exp\left(\frac{-\hbar\omega}{kT}\right) \times d(\hbar\omega) \right] \quad (5)$$

To avoid the dependence on the choice of model for the intrinsic carrier density, instead of placing the emphasis on determining values of the radiative recombination coefficient $B(T)$, we consider the more general parameter $B(T) \times n_i^2$, which is the product of the radiative recombination coefficient and the square of the intrinsic carrier density.

$$B(T) \times n_i^2 = \frac{1}{\pi^2\hbar^3 c_0^2} \int_0^\infty \left[n^2 \times (\hbar\omega)^2 \times \alpha_{BB}(\hbar\omega, T) \times \exp\left(\frac{-\hbar\omega}{kT}\right) \times d(\hbar\omega) \right] \quad (6)$$

where c_o is the speed of light in vacuum, k is Boltzmann's constant, T is the absolute temperature of the sample, and n is the refractive index of $CH_3NH_3PbI_3$.

From the temperature-dependent absorption coefficient values, we calculate $B(T) \times n_i^2$ as a function of temperature.[22,32] In eq 6, the refractive index n of $CH_3NH_3PbI_3$ is measured with an ellipsometer at room temperature. Since the refractive indices of $CH_3NH_3PbI_3$ at other temperatures are not yet known, we use the room temperature n to calculate $B(T) \times n_i^2$ for all temperatures. This is a reasonable assumption, as the impact of the temperature dependence of refractive index is negligible compared to the impact of other temperature dependent parameters. We plot $B(T) \times n_i^2$ as a function of temperature in Figure 5, where a fifth order polynomial function has been applied to fit the data points.[22,32] This fifth-order polynomial function can be used to calculate the absolute $B(T)$ when used in conjunction with a known intrinsic carrier density model.

$$\log_{10}[B(T) \times n_i^2] = -254.91 + 3.75 \times T - 0.024T^2 + 8.45 \times 10^{-5} \times T^3 - 1.49 \times 10^{-7} \times T^4 + 1.34 \times 10^{-10} \times T^5$$

In summary, the fundamental relationship between band-to-band absorptance and PL is used to determine the absorption coefficient of $CH_3NH_3PbI_3$ perovskite film at room temperature (295 K) for wavelengths from 675 to 1400 nm. Absorption coefficients of $CH_3NH_3PbI_3$ as small as 10^{-14}cm^{-1} are detected at room temperature. Knowledge of such data is a key piece of information to understand to what extent perovskite solar cells may suffer from parasitic absorption, which, in turn, is important for applications in tandem solar cells. The temperature-dependent $\alpha_{BB}(\hbar\omega)$ of $CH_3NH_3PbI_3$ perovskite films is also obtained with the same technique over a temperature range of 80−360 K. Based on $\alpha_{BB}(\hbar\omega)$ values extracted from the PLS at various temperatures, the product of radiative recombination coefficient and square of the intrinsic carrier density $B(T) \times n_i^2$ of $CH_3NH_3PbI_3$ perovskite are also calculated, and a fifth-order polynomial relation is provided.

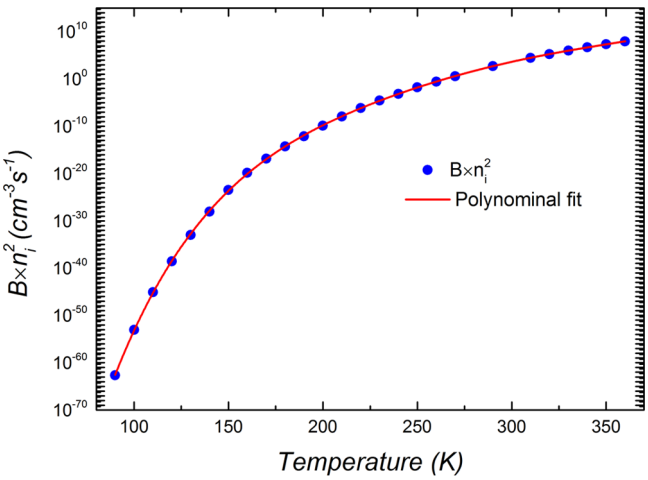

Figure 5. Product of the radiative recombination coefficient and the square of the intrinsic carrier density $B(T) \times n_i^2$ plotted as a function of temperature (blue solid circles). A fifth-order polynomial function is used to fit the experimental values (red line).

■ ASSOCIATED CONTENT

Supporting Information

Additional figures, including a comparison of absorption coefficient calculated using method 1 (eqs 2 and 3) and method 2 (eq 4), a figure showing the temperature dependence of the band edge of $CH_3NH_3PbI_3$, and the tabulated band to band absorption coefficient of $CH_3NH_3PbI_3$ perovskite film extracted from PLS at room temperature from 675 to 1400 nm. This material is available free of charge via the Internet at http://pubs.acs.org.

■ AUTHOR INFORMATION

Corresponding Author

*E-mail: kylie.catchpole@anu.edu.au.

Notes

The authors declare no competing financial interest.

■ ACKNOWLEDGMENTS

The authors thank Prof. Uwe Rau from IEK-5 Forschungszentrum Jülich, Germany, for helpful discussion. This Program has been supported by the Australian Government through the Australian Renewable Energy Agency (ARENA). Responsibility for the views, information, or advice expressed herein is not accepted by the Australian Government. K.R.C. is grateful for the support of a Future Fellowship from the Australian Research Council.

DOI: 10.1021/acs.jpclett.5b00044
J. Phys. Chem. Lett. 2015, 6, 767−772

REFERENCES

(1) Kojima, A.; Teshima, K.; Shirai, Y.; Miyasaka, T. Organometal Halide Perovskites as Visible-Light Sensitizers for Photovoltaic Cells. *J. Am. Chem. Soc.* **2009**, *131*, 6050−6051.

(2) Service, R. F. Energy technology: Perovskite Solar Cells Keep on Surging. *Science* **2014**, *344*, 458.

(3) NREL http://www.nrel.gov/ncpv/images/efficiency_chart.jpg.

(4) Snaith, H. J. Perovskites: The Emergence of a New Era for Low-Cost, High-Efficiency Solar Cells. *J. Phys. Chem. Lett.* **2013**, *4*, 3623−3630.

(5) De Wolf, S.; Holovsky, J.; Moon, S.-J.; Löper, P.; Niesen, B.; Ledinsky, M.; Haug, F.-J.; Yum, J.-H.; Ballif, C. Organometallic Halide Perovskites: Sharp Optical Absorption Edge and Its Relation to Photovoltaic Performance. *J. Phys. Chem. Lett.* **2014**, *5*, 1035−1039.

(6) Xing, G.; Mathews, N.; Sun, S.; Lim, S. S.; Lam, Y. M.; Grätzel, M.; Mhaisalkar, S.; Sum, T. C. Long-Range Balanced Electron- and Hole-Transport Lengths in Organic-Inorganic $CH_3NH_3PbI_3$. *Science.* **2013**, *342*, 344−347.

(7) White, T. P.; Lal, N. N.; Catchpole, K. R. Tandem Solar Cells Based on High-Efficiency c-Si Bottom Cells: Top Cell Requirements for >30% Efficiency. *IEEE J. Photovoltaics* **2014**, *4*, 208−214.

(8) Lal, N. N.; White, T. P.; Catchpole, K. R. Optics and Light Trapping for Tandem Solar Cells on Silicon. *IEEE J. Photovoltaics* **2014**, *4*, 1380−1386.

(9) Löper, P.; Moon, S.-J.; Martin de Nicolas, S.; Niesen, B.; Ledinsky, M.; Nicolay, S.; Bailat, J.; Yum, J.-H.; De Wolf, S.; Ballif, C. Organic−Inorganic Halide Perovskite/Crystalline Silicon Four-Terminal Tandem Solar Cells. *Phys. Chem. Chem. Phys.* **2015**, *17*, 1619−1629.

(10) Lin, Q.; Armin, A.; Nagiri, R. C. R.; Burn, P. L.; Meredith, P. Electro-optics of Perovskite Solar Cells. *Nat. Photonics* **2014**, *9*, 106−112.

(11) Löper, P.; Stuckelberger, M.; Niesen, B.; Werner, J.; Filipič, M.; Moon, S.-J.; Yum, J.-H.; Topič, M.; De Wolf, S.; Ballif, C. Complex Refractive Index Spectra of $CH_3NH_3PbI_3$ Perovskite Thin Films Determined by Spectroscopic Ellipsometry and Spectrophotometry. *J. Phys. Chem. Lett.* **2014**, *6*, 66−71.

(12) Schneider, B. W.; Lal, N. N.; Baker-Finch, S.; White, T. P. Pyramidal Surface Textures for Light Trapping and Antireflection in Perovskite-on-Silicon Tandem Solar Cells. *Opt. Express.* **2014**, *22*, A1422−A1430.

(13) Trupke, T.; Bardos, R. A.; Schubert, M. C.; Warta, W. Photoluminescence Imaging of Silicon Wafers. *Appl. Phys. Lett.* **2006**, *89*, 044107−044107−3.

(14) Gundel, P.; Schubert, M. C.; Warta, W. Simultaneous Stress and Defect Luminescence Study on Silicon. *Phys. Status Solidi A* **2010**, *207*, 436−441.

(15) Daub, E.; Würfel, P. Ultralow Values of the Absorption Coefficient of Si Obtained from Luminescence. *Phys. Rev. Lett.* **1995**, *74*, 1020−1023.

(16) Trupke, T.; Daub, E.; Würfel, P. Absorptivity of Silicon Solar Cells Obtained from Luminescence. *Sol. Energy Mater. Sol. Cells.* **1998**, *53*, 103−114.

(17) Barugkin, C.; Wan, Y.; Macdonald, D.; Catchpole, K. R. Evaluating Plasmonic Light Trapping with Photoluminescence. *IEEE J. Photovoltaics* **2013**, *3*, 1292−1297.

(18) Nguyen, H. T.; Rougieux, F. E.; Mitchell, B.; Macdonald, D. Temperature Dependence of the Band−Band Absorption Coefficient in Crystalline Silicon from Photoluminescence. *J. Appl. Phys.* **2014**, *115*, 043710−043710−8.

(19) Wurfel, P. The Chemical Potential of Radiation. *J. Phys. C: Solid State Phys.* **1982**, *15*, 3967−3985.

(20) Feuerbacher, B.; Wurfel, P. Verification of a Generalised Planck Law by Investigation of the Emission from GaAs Luminescent Diodes. *J. Phys.: Condens. Matter.* **1990**, *2*, 3803−3810.

(21) Schick, K.; Daub, E.; Finkbeiner, S.; Würfel, P. Verification of a Generalized Planck Law for Luminescence Radiation from Silicon Solar Cells. *Appl. Phys. A: Mater. Sci. Process.* **1992**, *54*, 109−114.

(22) Trupke, T.; Green, M. A.; Würfel, P.; Altermatt, P. P.; Wang, A.; Zhao, J.; Corkish, R. Temperature Dependence of The Radiative Recombination Coefficient of Intrinsic Crystalline Silicon. *J. Appl. Phys.* **2003**, *94*, 4930−4937.

(23) Würfel, P.; Trupke, T.; Puzzer, T.; Schäffer, E.; Warta, W.; Glunz, S. W. Diffusion Lengths of Silicon Solar Cells from Luminescence Images. *J. Appl. Phys.* **2007**, *101*, 123110−123110−10.

(24) Nguyen, H. T.; Rougieux, F. E.; Baker-Finch, S. C.; Macdonald, D. Impact of Carrier Profile and Rear-Side Reflection on Photoluminescence Spectra in Planar Crystalline Silicon Wafers at Different Temperatures. *IEEE J. Photovoltaics* **2014**, *5*, 77−81.

(25) Ledinský, M.; Löper, P.; Niesen, B.; Holovský, J.; Moon, S.-J.; Yum, J.-H.; De Wolf, S.; Fejfar, A.; Ballif, C. Raman Spectroscopy of Organic−Inorganic Halide Perovskites. *J. Phys. Chem. Lett.* **2015**, 401−406.

(26) Stoumpos, C. C.; Malliakas, C. D.; Kanatzidis, M. G. Semiconducting Tin and Lead Iodide Perovskites with Organic Cations: Phase Transitions, High Mobilities, and Near-Infrared Photoluminescent Properties. *Inorg. Chem.* **2013**, *52*, 9019−9038.

(27) Green, M. A.; Ho-Baillie, A.; Snaith, H. J. The Emergence of Perovskite Solar Cells. *Nat. Photonics* **2014**, *8*, 506−514.

(28) Green, M. A. Self-Consistent Optical Parameters of Intrinsic Silicon at 300 K Including Temperature Coefficients. *Sol. Energy Mater. Sol. Cells.* **2008**, *92*, 1305−1310.

(29) Green, M. A.; Keevers, M. J. Optical Properties of Intrinsic Silicon at 300 K. *Prog. Photovoltaics Res. Appl.* **1995**, *3*, 189−192.

(30) Wu, K.; Bera, A.; Ma, C.; Du, Y.; Yang, Y.; Li, L.; Wu, T. Temperature-Dependent Ecitonic Photoluminescence of Hybrid Organometal Halide Perovskite Films. *Phys. Chem. Chem. Phys.* **2014**, *16*, 22476−22481.

(31) Altermatt, P. P.; Geelhaar, F.; Trupke, T.; Dai, X.; Neisser, A.; Daub, E. Injection Dependence of Spontaneous Radiative Recombination in Crystalline Silicon: Experimental Verification and Theoretical Analysis. *Appl. Phys. Lett.* **2006**, *88*, 261901−261901−3.

(32) Nguyen, H. T.; Baker-Finch, S. C.; MacDonald, D. Temperature Dependence of the Radiative Recombination Coefficient in Crystalline Silicon from Spectral Photoluminescence. *Appl. Phys. Lett.* **2014**, *104*, 112105-1−112105-3.

DOI: 10.1021/acs.jpclett.5b00044
J. Phys. Chem. Lett. 2015, 6, 767−772